an industrial robot with elasticity, as reported in the works [31], [32], [33]. Such model has also been used to reproduce the dynamics of an ABB IRB6600 industrial robot in [4]. The dynamics of the system is:

$$\begin{array}{l} J_1\ddot{q}_1 = k(q_2 - q_1) + k(q_2 - q_1)^3 + u \\ J_2\ddot{q}_2 = -k(q_2 - q_1) - k(q_2 - q_1)^3 \end{array} \quad (23)$$

in which u is the motor torque applied to the first mass of inertia J_1, while the second mass has inertia J_2. The speed of rotation of the mass will be indicated as $\dot{q}_1$ or ω_1 for the first mass and $\dot{q}_2$ or ω_2 for the second mass. If $J_1 = J_2 = 1$, the dynamics of the system in eq. 23 can be rewritten as:

$$\dot{\mathbf{x}} = \begin{bmatrix} k(q_2 - q_1) + k(q_2 - q_1)^3 + u \\ -k(q_2 - q_1) - k(q_2 - q_1) \\ \omega_1 \\ \omega_2 \end{bmatrix} \quad (24)$$

The procedure shown in section 2 cannot be directly applied in this case if constraints are to included in the problem. This is due to the fact that the application of Pontryagin's minimum principle requires for the Hamltionian to be differentiable in time with continuous derivatives in $\mathbf{x}(t)$ and $\Lambda(t)$, and therefore hard constraints cannot be applied using a saturation function. The proposed solution to this situation is the use of a smoothing function.

First, let us take into consideration the nominal solution of the trajectory planning problem without constraints. The Hamiltonian of the systems for the minimum effort solution is:

$$\begin{array}{l} \mathcal{H} = \lambda_3\omega_1 - \lambda_1(k(q_1 - q_2) - u + k(q_1 - q_2)^3) \\ +\lambda_4\omega_2 + \lambda_2(k(q_1 - q_2) + k(q_1 - q_2)^3) + \dfrac{u^2}{2} \end{array} \quad (25)$$

and the application of the condition in eq. (5) leads to:

$$\frac{\partial \mathcal{H}}{\partial u} = u + \lambda_1 \quad (26)$$

The last equation highlights that the optimal control action is $u^* = -\lambda_1$, therefore the system of ordinary differential equations to be solved is:

$$\dot{\mathbf{y}}^* = \begin{bmatrix} -\lambda_1 - k(q_1 - q_2) - k(q_1 - q_2)^3 \\ k(q_1 - q_2) + k(q_1 - q_2)^3 \\ \omega_1 \\ \omega_2 \\ -\lambda_3 \\ -\lambda_4 \\ k(\lambda_1 - \lambda_2)(3{q_1}^2 - 6q_1q_2 + 3{q_2}^2 + 1) \\ -k(\lambda_1 - \lambda_2)(3{q_1}^2 - 6q_1q_2 + 3{q_2}^2 + 1) \end{bmatrix} \quad (27)$$

The problem defined in the last equation is unconstrained. A simple solution can be found to constrain one or more of the state and lagrangians through the use of a smooth saturation function. The definition of the saturation function is:

$$sat(s, \gamma) = \begin{cases} s, & |s| < \gamma \\ \gamma sign(s), & |s| > \gamma \end{cases} \quad (28)$$

which can be approximated as:

$$SAT(s, \gamma, \nu) = \frac{\gamma}{2}\left(\sqrt{\nu + \left(\frac{s}{\gamma} + 1\right)^2} - \sqrt{\nu + \left(\frac{s}{\gamma} - 1\right)^2}\right) \quad (29)$$

This approximation has been introduced and used by Avvakumov in [34] for the constrained solution of boundary value problem. The quality of the approximation is inversely proportional to the constant positive parameter ν. Simple numerical evaluations show that a sufficiently good approximation can be achieved for $\nu = 1e - 6$: for this value of ν the approximation error, i.e. the difference between the ideal saturation function and its approximating function, is less than $2e - 4$ for $\gamma = 1$. The application of this approximated saturation function to the problem stated in eq. (27) requires simply to substitute in it λ_1 with the expression in eq. (29). This allows to limit λ_1, and therefore u^*, in the range $u \in [-\gamma, \gamma]$.

In the following the results of the computation of the trajectory planning algorithm are shown. The boundary conditions are set in order to bring the two masses from the initial position $q_1(t = 0) = 0.1$ rad and $q_2(t = 0) = 0.1$ rad to $q_1(t = t_f) = q_2(t = t_f) = 0$ rad with initial and final speed equal to zero. Therefore a rest-to-rest motion is planned. In this case the total execution time is chosen to be $t_f = 2$ s. The values of u is limited in the range $[-2.5, 2.5]$ Nm for the constrained solution.

The control action u is for the unconstrained and constrained case is shown in figure 8. The planned trajectory is shown in Fig. 9. In particular, it can be seen that the inclusion of constraints allows to precisely limit the amplitude of u: as imposed in the definition of the optimization problem, the torque provided by the motor never exceeds the prescribed value of 2.5 Nm. This result has been obtained with $\nu = 1 \times 10^{-9}$. It has been verified numerically that lowering the value of ν does not improve the quality of the solution. The actual trajectories for the unconstrained and constrained solutions are similar to each other, as it can be seen in Figure 5. In the constrained case the first mass achieves a slightly higher speed than in the nominal case, which is a direct effect of the torque limitation.

The application of the control profile $u(t)$ shown in figure 8 to a nominal plant, i.e. to a plant in which the spring stiffness is proportional to $k = 1\ Nm/rad$ is shown in figure 10, which shows that zero residual vibration can be achieved also in the presence of constraints.

On the other hand if a perturbed plant is taken into consideration, and in particular if the value of k is increased by 30%, the application of the feedforward torque profile

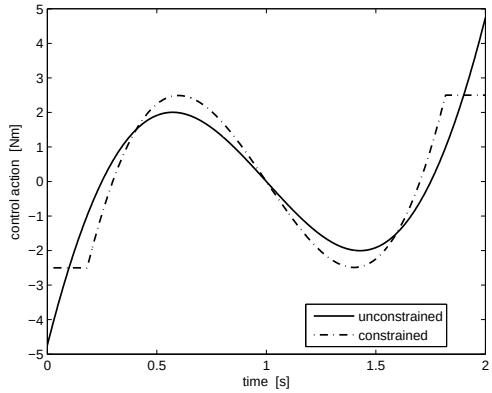

Fig. 8. Control action for the nominal case: constrained and unconstrained solutions

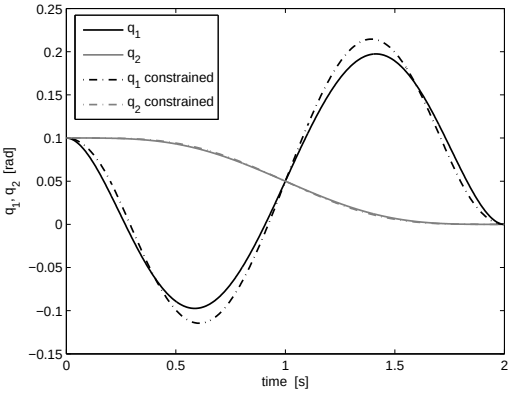

Fig. 9. Joint trajectory for the nominal case: constrained and unconstrained solution

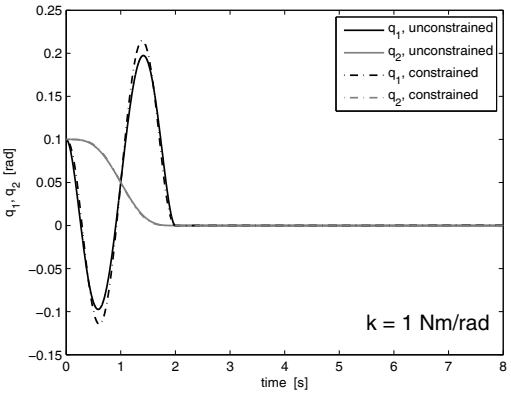

Fig. 10. Joint trajectory for the nominal case: constrained and unconstrained solution

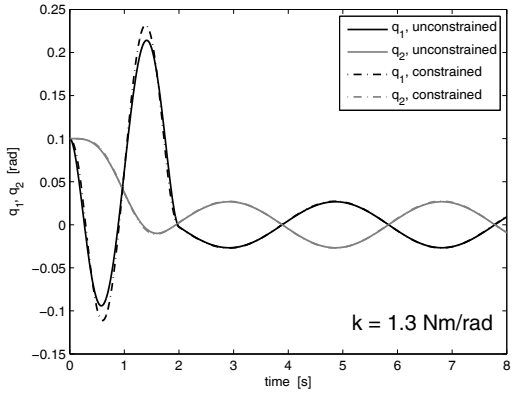

Fig. 11. Joint trajectory for the nominal case: constrained and unconstrained solution

leads to the results show in figure 11. The analysis of this plot highlights the presence of noticeable residual vibration after motion completion, i.e. after 2 seconds from the simulation starting point. The peak-to-peak amplitude of residual vibrations is equal to $0.056\ rad$, i.e. more than half of the prescribed mass displacement for the whole motion. A more complete evaluation of the residual vibration for the constrained and the unconstrained solution is shown in figure 12 in terms of residual energy of the system at time $t = t_f$. The residual energy E is evaluated as the sum of the kinetic energy T and the elastic energy U as:

$$E = T + U \tag{30}$$

in which the kinetic energy is simply:

$$T = \frac{1}{2}(J_1\omega_1^2 + J_2\omega_2^2) \tag{31}$$

while the elastic energy is:

$$\begin{aligned} U = \int_0^{\Delta q^*} F\Delta q d\Delta q = \int_0^{\Delta q^*} (k\Delta q + k^3\Delta q) \\ = k\left(\frac{1}{2}\Delta q^{*2} + \frac{1}{4}\Delta q^{*2}\right) \end{aligned} \tag{32}$$

The residual energy is used in this section as a measurement of the robustness of the outcome of the trajectory planning algorithm. Under nominal conditions,i.e. without any perturbations, the residual energy of the system must be equal to zero, since the prescribed right-side boundary condition is $\mathbf{x}(t_f) = \beta = [0, 0, 0, 0]^T$. Any deviation from this value can be measured through the use of the residual energy of the system, which can be seen as a norm of the vector $\mathbf{x}(t_d)$.

Figure 12 shows how the value of of the elastic constant k affects the value of residual energy after task completion. It can be seen in figure 12 that the residual energy is equal

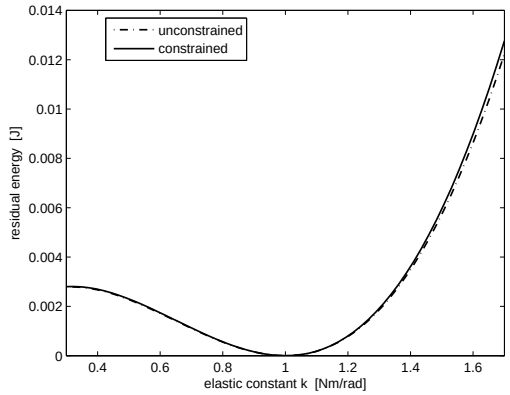

Fig. 12. Residual energy: unconstrained and constrained solutions, nominal trajectory with $k \in [0.3, 1.7]\ Nm/rad$

to zero only for $k = 1\ N/m$, and that the residual energy quickly grows with increasing and decreasing values of k. This applies with very similar trends for both the constrained and the unconstrained solutions. The following part of the paper will show how the use of sensitivity functions allows to improve the robustness of the computed trajectories with respect to variations of the elastic constant k.

As shown in the case of the simple mass-spring system, the robustness of the solution of the trajectory generation problem can be improved by imposing additional boundary condition on the sensitivity function in the optimization problem definition. Using the same procedure and applying it to the elastic joint case, the sensitivity equations can be computed as:

$$\begin{aligned}
&\frac{d}{dt}\left(\frac{\partial \omega_1}{\partial k}\right) = (q_2 - q_1) + (q_2 - q_1)^3 + \\
&\quad + k\left(\frac{\partial q_2}{\partial k} - \frac{\partial q_1}{\partial k}\right)^3 + 3k\left(\frac{\partial q_2}{\partial k} - \frac{\partial q_1}{\partial k}\right)(q_2 - q_1)^2; \\
&\frac{d}{dt}\left(\frac{\omega_2}{\partial k}\right) = -(q_2 - q_1) - (q_2 - q_1)^3 \\
&\quad - k\left(\frac{\partial q_2}{\partial k} - \frac{\partial q_1}{\partial k}\right)^3 - 3k\left(\frac{\partial q_2}{\partial k} - \frac{\partial q_1}{\partial k}\right)(q_2 - q_1)^2; \\
&\frac{d}{dt}\left(\frac{\partial q_1}{\partial k}\right) = \frac{\partial \omega_1}{\partial k}; \\
&\frac{d}{dt}\left(\frac{q_2}{\partial k}\right) = \frac{\partial \omega_2}{\partial k};
\end{aligned} \tag{33}$$

This choice of parametric uncertainty can be practically useful in all the cases in which the elastic constant of the flexible joint cannot be estimated with sufficient accuracy, or in the cases in which variations of the elastic constant are not described by the dynamic model used for trajectory planning. The Hamiltonian of the system is therefore:

$$\begin{aligned}
\mathcal{H} &= \lambda_3\omega_1 - \lambda_1\left(k(q_1 - q_2) - u + k(q_1 - q_2)^3\right) \\
&\quad + \lambda_4\omega_2 + \lambda_7\frac{\partial \omega_1}{\partial k} + \lambda_8\frac{\partial \omega_2}{\partial k} \\
&\quad - \lambda_5\left(q_1 - q_2 + (q_1 + q_2)^2 + k\left(\frac{\partial q_1}{\partial k} - \frac{\partial q_2}{\partial k}\right)\right) \\
&\quad - 3\lambda_5 k(q_1 - q_2)^2\left(\frac{\partial q_1}{\partial k} - \frac{\partial q_2}{\partial k}\right) \\
&\quad + \lambda_6\left(q_1 - q_2 + (q_1 + q_2)^2 + k\left(\frac{\partial q_1}{\partial k} - \frac{\partial q_2}{\partial k}\right)\right) \\
&\quad + 3\lambda_6 k(q_1 - q_2)^2\left(\frac{\partial q_1}{\partial k} - \frac{\partial q_2}{\partial k}\right) \\
&\quad + \lambda_2\left(k(q_1 - q_2) + k(q_1 - q_2)^3\right) + \frac{u^2}{2}
\end{aligned} \tag{34}$$

and the application of the condition of eq. (5) leads to the optimal control:

$$u^* = -\lambda_1 \tag{35}$$

Equations above refer to the unconstrained solution: hard limits on the control action can be achieved by direct substitution of λ_1 with the smoothing function defined in eq. (25). The complete formulation is here omitted due to the limited space availability. Boundary conditions are the same used for the nominal case, with the obvious addition of constraints on the sensitivity functions. The total execution time has been increased to $3.75\ s$ in order to produce a trajectory with the same peak torque as the nominal one. The control profile evaluated through the solution of the augmented TPBVP is shown in fig. 13: as in the previously shown nominal case (see fig. 8) the smoothing technique allows to precisely limit the control action in the range $[-2.5, 2.5]\ Nm$. The same solution shown in terms of joint positions is shown in figure 14: its accuracy is confirmed by the results available in figure 15, which shows the results of the feedforward application of the planned control profile. The absence of noticeable residual vibration highlights the accuracy of the solution when a nominal plant, therefore with $k = 1\ Nm$ is taken into account. The application of the same control profile to a plant with a stiffness values increased by 30% is reported in figure 16: the residual vibration has a peak-to-peak amplitude of 0.0161 rad, which is 3.4 times smaller than the same value obtained under the same conditions by the nominal trajectory, as visible from the comparison between figures 16 and 11.

A comparison in terms of residual energy between the nominal and robust solutions, with and without the application of constraints, is shown in figure 17. The figure shows how a change in the value of the elastic constant k for a $\pm 30\%$ variation influences the residual energy after motion completion. The analysis of the data presented in

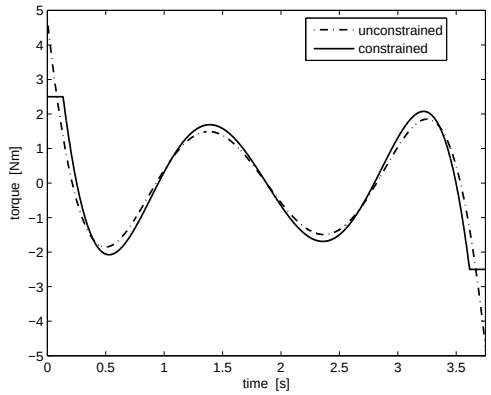

Fig. 13. Robust solution: torque for unconstrained and constrained solutions

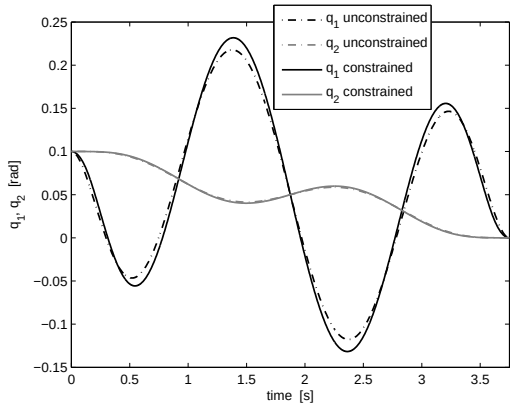

Fig. 14. Planned trajectory: robust solutions

this graph allows to conclude that, for the case under consideration, the inclusion of robustness conditions allows to significantly reduce the sensitivity of the plant to parametric mismatches, and that the inclusion of hard constraints on the actuator effort has a very limited effect on the robustness properties of the planned trajectory.

V. Conclusions

In this paper the problem of generating model-based robust trajectories for nonlinear mechatronic systems is dealt with. The work proposed a method based on the use of sensitivity function which allows to improve the robustness to parametric mismatches to augment the classic approach based on the solution of a two-point boundary value problem. Also the problem of including constraints is dealt with, using an accurate smoothing technique. The effectiveness of the approach is tested on two benchmark problem: a nonlinear mass-spring system and a nonlinear flexible joint manipulator. Results highlight that the proposed approach can lead to a sensible improvement to parametric mismatches of the planning trajectory, and that constraints can be included with accuracy without affecting the parametric robustness

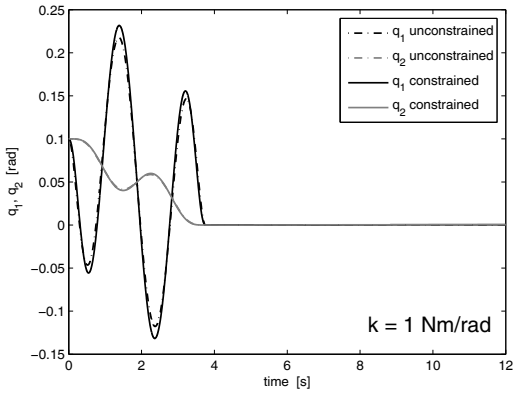

Fig. 15. Joint trajectories for the nominal case: robust solutions

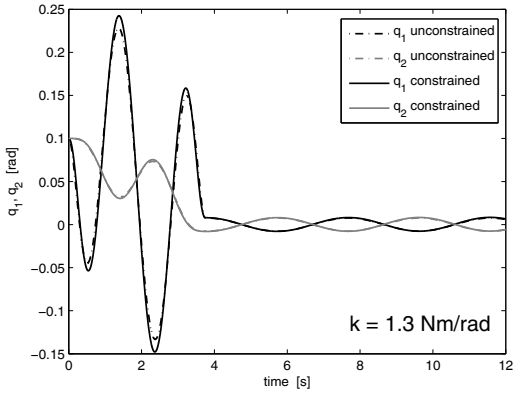

Fig. 16. Joint trajectories for the perturbed plant ($k = 1.3\ Nm/rad$): robust solutions

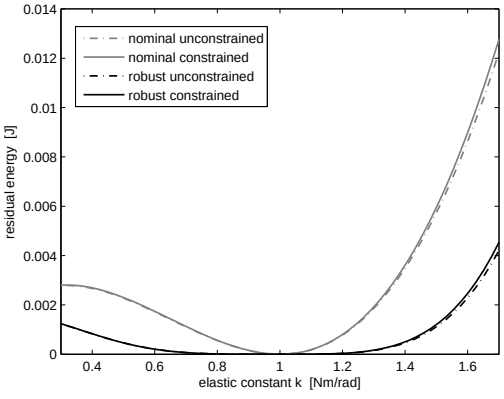

Fig. 17. Comparison of the residual energy between nominal, nominal constrained, robust and robust constrained solutions

of the solution.

References

[1] A. De Luca, G. Di Giovanni, Rest-to-rest motion of a two-link robot with a flexible forearm, in: Advanced Intelligent Mechatronics, 2001. Proceedings. 2001 IEEE/ASME International Conference on, Vol. 2, IEEE, 2001, pp. 929–935.

[2] P. Gallina, A. Trevisani, Synthesis and experimental validation of a delayed reference controller for active vibration suppression in mechanical systems, Journal of applied mechanics 72 (4) (2005) 623–627.

[3] P. Boscariol, V. Zanotto, Design of a controller for trajectory tracking for compliant mechanisms with effective vibration suppression, Robotica 30 (01) (2012) 15–29.

[4] S. Moberg, E. Wernholt, S. Hanssen, T. Brogårdh, Modeling and parameter estimation of robot manipulators using extended flexible joint models, Journal of Dynamic Systems, Measurement, and Control 136 (3) (2014) 031005.

[5] R. Vidoni, A. Gasparetto, M. Giovagnoni, Design and implementation of an erls-based 3-d dynamic formulation for flexible-link robots, Robotics and Computer-Integrated Manufacturing 29 (2) (2013) 273–282.

[6] R. Vidoni, A. Gasparetto, M. Giovagnoni, A method for modeling of three-dimensional flexible mechanisms based on an equivalent rigid-link system, Journal of Vibration and Control 20 (4) (2014) 483–500.

[7] A. A. Ata, Optimal trajectory planning of manipulators: a review, Journal of Engineering Science and Technology 2 (1) (2007) 32–54.

[8] A. Gasparetto, P. Boscariol, A. Lanzutti, R. Vidoni, Trajectory planning in robotics, Mathematics in Computer Science (2012) 1–11.

[9] P. Boscariol, A. Gasparetto, Model-based trajectory planning for flexible-link mechanisms with bounded jerk, Robotics and Computer-Integrated Manufacturing 29 (2013) 90–99.

[10] P. Boscariol, A. Gasparetto, R. Vidoni, A. Romano, A model-based trajectory planning approach for flexible-link mechanisms, in: Mechatronics (ICM), 2013 IEEE International Conference on, IEEE, 2013, pp. 219–224.

[11] R. Caracciolo, D. Richiedei, A. Trevisani, Experimental validation of a model-based robust controller for multi-body mechanisms with flexible links, Multibody System Dynamics 20 (2) (2008) 129–145.

[12] M. Boryga, A. Graboś, Planning of manipulator motion trajectory with higher-degree polynomials use, Mechanism and machine theory 44 (7) (2009) 1400–1419.

[13] P. Boscariol, A. Gasparetto, R. Vidoni, Jerk-continuous trajectories for cyclic tasks, in: ASME 2012 International Design Engineering Technical Conferences and Computers and Information in Engineering Conference, American Society of Mechanical Engineers, 2012, pp. 1277–1286.

[14] C. Louembet, F. Cazaurang, A. Zolghadri, Motion planning for flat systems using positive b-splines: An lmi approach, Automatica 46 (8) (2010) 1305–1309.

[15] P. Boscariol, A. Gasparetto, R. Vidoni, Planning continuous-jerk trajectories for industrial manipulators, in: ASME 2012 11th Biennial Conference on Engineering Systems Design and Analysis, American Society of Mechanical Engineers, 2012, pp. 127–136.

[16] D. Balkcom, M. Mason, Time optimal trajectories for bounded velocity differential drive vehicles, The International Journal of Robotics Research 21 (3) (2002) 199–217.

[17] O. Dahl, Path constrained motion optimization for rigid and flexible joint robots, in: International Conference on Robotics and Automation, Vol. 2, IEEE, 1993, pp. 223–229.

[18] M. Korayem, H. R. Nohooji, A. Nikoobin, Optimal motion generating of nonholonomic manipulators with elastic revolute joints in generalized point-to-point task, International journal of advanced design and manufacturing technology 3 (2) (2010) 1–9.

[19] A. Abe, Trajectory planning for residual vibration suppression of a two-link rigid-flexible manipulator considering large deformation, Mechanism and Machine Theory 44 (9) (2009) 1627–1639.

[20] M. Korayem, A. Nikoobin, V. Azimirad, Trajectory optimization of flexible link manipulators in point-to-point motion, Robotica 27 (6) (2009) 825–840.

[21] D. Gallardo, O. Colomina, F. Flórez, R. Rizo, A genetic algorithm for robust motion planning, Tasks and Methods in Applied Artificial Intelligence (1998) 115–121.

[22] K. G. Shin, N. D. McKay, Robust trajectory planning for robotic manipulators under payload uncertainties, Automatic Control, IEEE Transactions on 32 (12) (1987) 1044–1054.

[23] B. Houska, Robust optimization of dynamic systems, Ph.D. thesis, PhD thesis, Katholieke Universiteit Leuven, 2011.(ISBN: 978-94-6018-394-2) (2011).

[24] T. Singh, Optimal reference shaping for dynamical systems: theory and applications, CRC PressI Llc, 2010.

[25] T. A. Hindle, T. Singh, Desensitized minimum power/jerk control profiles for rest-to-rest maneuvers, in: American Control Conference, 2000. Proceedings of the 2000, Vol. 5, IEEE, 2000, pp. 3064–3068.

[26] R. Kased, T. Singh, Rest-to-rest motion of an experimental flexible structure subject to friction: Linear programming approach, in: AIAA Guidance, Navigation and Control Conference, San Francisco, CA, 2005.

[27] L. Pontryagin, R. Gamkrelidze, The mathematical theory of optimal processes, Vol. 4, CRC, 1986.

[28] L. Shampine, I. Gladwell, S. Thompson, Solving ODEs with MATLAB, Cambridge University Press, 2003.

[29] R. W. Holsapple, A modified simple shooting method for solving two-point boundary value problems.

[30] G. Boschetti, R. Caracciolo, D. Richiedei, A. Trevisani, A non-time based controller for load swing damping and path-tracking in robotic cranes, Journal of Intelligent & Robotic Systems (2014) 1–17.

[31] S. Moberg, On modeling and control of flexible manipulators, Ph.D. thesis, Department of Electrical Engineering, Linkping University, Sweden (2007).

[32] P. Axelsson, Evaluation of six different sensor fusion methods for an industrial robot using experimental data, in: 10th International IFAC Symposium on Robot Control, Dubrovnik, Croatia, 2012.

[33] P. Axelsson, M. Norrlöf, E. Wernholt, F. Gustafsson, Extended kalman filter applied to industrial manipulators, in: Proceedings of Reglermöte 2010, Lund, Sweden, 2010.

[34] S. Avvakumov, Y. N. Kiselev, Boundary value problem for ordinary differential equations with applications to optimal control, Spectral and Evolution Problems 2000 10.